Sasaki, K., Ishizaka, T., Suzuki, T., and Saito, Y. (1988) Determination of tri-*n*-butyltin and di-*n*-butyltin compounds in fish by gas chromatography with flame photometric detection, *Journal of the Association of Official Analytical Chemists*, 71, 360–3.

Scadding, S.R. (1990) Effects of tributyltin oxide on the skeletal structures of developing and regenerating limbs of the axolotl larvae, *Ambystoma mexicanum*, *Bulletin of Environmental Contamination and Toxicology*, 45, 574–81.

Schardein, J. (2000) Hormones and hormonal antagonists, in *Chemically Induced Birth Defects*, 3rd ed., revised and expanded, Marcel Dekker, New York.

Short, J.W. and Thrower, F.P. (1986) Accumulation of butyltins in muscle tissue of chinook salmon reared in sea pens treated with tri-*n*-butyltin, *Marine Pollution Bulletin*, 17, 542–5.

Smith, B.S. (1981a). Male characteristics on female mud snails caused by antifouling paints, *Journal of Applied Toxicology*, 1, 22–5.

Smith, B.S. (1981b). Tributyltin compounds induce male characteristics on female mud snails *Nassarius oboletus = Ilyanasa oboleta*, *Journal of Applied Toxicology*, 1, 141–4.

Snoeij, N.J., Penninks, A.H., and Seinen, W. (1987) Biological activity of organotin compounds—an overview, *Environmental Research*, 44, 335–53.

Snow, R.L. and Hays, R.L. (1983) Phasic distribution of seminiferous tubules in rats treated with triphenyltin compounds, *Bulletin of Environmental Contamination and Toxicology*, 31, 658–65.

Spencer, F. and Sing, L.T. (1982) Reproductive responses to rotenone during decidualized pseudogestation and gestation in rats, *Bulletin of Environmental Contamination and Toxicology*, 28, 360–8.

Spooner, N., Gibbs, P.E., Bryan, G.W., and Goad, L.J. (1991) The effect of tributyltin upon steroid titers in the female dogwhelk, *Nucella lapillus*, and the development of imposex, *Marine Environmental Research*, 32, 37–49.

Strmac, M. and Braunbeck, T. (1999) Effects of triphenyltin acetate on survival, hatching success, and liver ultrastructure of early life stages of zebrafish (*Danio rerio*), *Ecotoxicology and Environmental Safety*, 44, 25–39.

Stroben, E., Oehlmann, J., and Bettin, C. (1991) TBT-induced imposex and role of steroids in marine snails, in *Proceedings Tenth World Meeting of the Organotin Environmental Programme Association*, Berlin, September, 68–73.

Suzuki, T., Matsuda, R., and Saito, Y. (1992) Molecular species of tri-*n*-butyltin compounds in marine products, *Journal of Agricultural and Food Chemistry*, 40, 1437–43.

Takahashi, T., Araki, A., Nomura, Y., Koga M., and Arizono, K. (2000) The occurrence of dual-gender imposex in Japanese freshwater crab, *Journal of Health Science*, 46, 376–9.

Toyoda, M., Sakai, H., Kobayashi, Y., Komatsu, M., Hoshino Y., Horie, M., Saeki, M., Hasegawa, Y., Tsuji, M., Kojima, M., Toyomura, K., Kumano, M., and Tanimura, A. (2000) Daily dietary intake of tributyltin, dibutyltin, triphenyltin and diphenyltin compounds according to a total diet study in Japanese population, *Shokuhin Eiseigaku Zasshi*, 41, 280–6 (in Japanese).

Tryphonas, H., Cooke, G.M., Caldwell, D., Bondy, G., Parenteau, M., Hayward, S., and Pulido, O. (2004) Oral (gavage), in utero and postnatal exposure of Sprague-Dawley rats to low doses of tributyltin chloride. Part II: Effects on the immune system, *Food and Chemical Toxicology*, 42, 221–235.

Tsuda, T., Inoue, T., Kojima, M., and Aoki, S. (1995) Daily intakes of tributyltin and triphenyltin comounds from meals, *Journal of AOAC International*, 78, 941–3.

Tsuda, T., Nakanishi, H., Aoki, S., and Takebayashi, J. (1987) Bioconcentration and metabolism of phenyltin chlorides in carp, *Water Research*, 21, 949–53.

Ueno, S., Susa, N., Furukawa, Y., Komatsu, Y., Koyama, S., and Suzuki, T. (1999) Butyltin and phenyltin compounds in some marine fishery products on the Japanese market, *Archives of Environmental Health*, 54, 20–5.

Waldock, M.J. and Thain, J.E. (1983) Shell thickening in Crassostrea gigas: organotin antifouling or sediment induced? *Marine Pollution Bulletin*, 14, 411–5.

Weis, J.S. and Kim, K. (1988) Tributyltin is a teratogen in producing deformities in limbs of the fiddler crab, *Uca pugilator*, *Archives of Environmental Contamination and Toxicology*, 17, 583–7.

Winek, C.L., Marks, M.J., Jr., Shanor, S.P., and Davis, E.R. (1978) Acute and subacute toxicology and safety evaluation of triphenyl tin hydroxide (Vancide KS), *Clinical Toxicology*, 13, 281–96.

Winship, K.A. (1988) Toxicity of tin and its compounds, *Adverse Drug Reactions and Acute Poisoning Reviews*, 7, 19–38.

World Health Organization (1980) Tin and Organotin Compounds: A Preliminary Review. *Environmental Health Criteria 15*, World Health Organization, Geneva.

World Health Organization (1992) Fentin, in *Pesticide Residues in Food 1991: Evaluations Part II Toxicology*, World Health Organization, Geneva. Online: http://www.inchem.org/documents/jmpr/jmpmono/v91pr11.htm (accessed 16 June 2004).

Yamabe, Y., Hoshino, A., Imura, N., Suzuki, T., and Himeno, S. (2000) Enhancement of androgen-dependent transcription and cell proliferation by tributyltin and triphenyltin in human prostate cancer cells, *Toxicology and Applied Pharmacology*, 169, 177–84.

Yonemoto, J., Shiraishi, H., and Soma, Y. (1993) In vitro assessment of teratogenic potential of organotin compounds using rat embryo limb bud cell cultures, *Toxicology Letters*, 66, 183–91.

SPRINGER REVIEWS

井上 達／井口泰泉 編

生体統御システムと内分泌撹乱

Springer
シュプリンガー・フェアラーク東京

6. 甲状腺ホルモン撹乱物質の生体作用の動物種差

加藤善久

6. 1. はじめに

ポリ塩化ビフェニル(PCB)は，食物連鎖を通して蓄積し，魚類，鳥類および多くの野生動物の組織のみならず，ヒトの血液，母乳，肝臓，脂肪組織などにも見出されている[1]．近年，PCBの曝露によって実験動物や野生生物だけでなく，ヒトにおいても甲状腺ホルモン(サイロキシン[T_4]，3,3',5-L-トリヨードサイロニン[T_3])の撹乱がひき起こされている[2]．ラットでは，いくつかのPCBの投与により血中T_4濃度の低下がひき起こされる[3,4]．一般に，PCBによるラットの血中T_4濃度の低下は，肝臓のUDP - グルクロノシルトランスフェラーゼ(UDP-GT)が誘導されることにより，T_4のグルクロン酸抱合体が増加し，その胆汁排泄が促進されることによると考えられている．しかし，PCBによる血中T_4濃度の低下と肝臓のT_4-UDP-GT活性の増加とは定量的に相関しない[3,4]など不明な点も多く，血中T_4濃度の低下メカニズムは十分に解明されていない．また，PCBの血中甲状腺ホルモンへの影響に関するほとんどの研究はラットを用いて行われたものであり，その低下作用における動物種差に関する研究は，ほとんど行われていない．筆者らはPCB投与による血中T_4濃度の低下メカニズムを明らかにするとともに，その低下のメカニズムに動物種差があるか否かを検討している．そこで，これまでの研究成果をここに紹介する．

6. 2. PCBの甲状腺ホルモンに対する作用：動物種差

筆者らは，種々の用量の2,2',4',5,5' - ペンタクロロビフェニル(ペンタCB)，2,2',3',4',5,6 - ヘキサクロロビフェニル(ヘキサCB)あるいはKanechlor-500(KC500，PCB製品であり，台湾油症の原因物質とされるPCB混合物)をマウスに投与し，投与量と血中総T_4濃度の関係から，マウスにおいて血中総T_4濃度を50％低下させる用量(ED_{50})を算出した．この用量をddY系マウス，Syrian系ハムスター，Wistar系ラットあるいはHartley系モルモットに投与した．血中総T_4濃度は，マウス，ハムスターおよびラットにペンタCB(11 mg/kg)を投与した後，マウスにヘキサCB(19 mg/kg)を投与した後，また4種の動物にKC500(37.5 mg/kg)を投与した後に，有意に低下した．血中総T_3濃度はマウスにペンタCBを投与したとき，あるいはモルモットにKC500を投与したときに有意に低下した．血中甲状腺刺激ホルモン濃度は，4種の動物にいずれのPCBを投与した場合にも変化しなかった．PCB投与による血中甲状腺ホルモン濃度の低下について，マウスで系統差のあることはわずかに報告されているが，このような動物種差に関する情報は乏しい．

6．3．血中T_4濃度の低下における肝臓UDP-GTの関与

一般に，PCBによるラット血中T_4濃度の低下の要因として，T_4のグルクロン酸抱合をはじめとするT_4の代謝系の促進が考えられる．そこで，3・2の動物のT_4-UDP-GT活性を測定した．T_4-UDP-GT活性は，マウスにヘキサCBを投与した後，あるいはモルモットにKC500を投与した後に有意に増加した．一方，ハムスターおよびラットに各PCBを投与したときには，この酵素活性は変化しなかった．さらに，KC500を投与した後，胆汁中T_4のグルクロン酸抱合体の排泄量は，ラットで有意に増加したが，マウス，ハムスター，モルモットでは変化しなかった．これらの結果から，マウスにヘキサCBを投与したときの血中T_4濃度の低下の要因には，肝臓のUDP-GTの誘導によるT_4の代謝促進を含む可能性がある．しかし，マウス，ハムスター，ラットおよびモルモットにペンタCBあるいはKC500を投与したときの血中T_4濃度の低下は，UDP-GTの誘導によるT_4の代謝促進では説明が困難である．

そこで，ラットにPCBを投与したときの血中T_4濃度の低下に，肝臓のUDP-GTによるT_4の代謝が関与しているか否かを明らかにするために，Wistar系ラットおよびGunnラット(遺伝的にUGT1サブファミリーを欠損したWistar系ラットの突然変異体)にペンタCB(112 mg/kg)あるいはKC500(100 mg/kg)を投与し，血中総T_4，遊離T_4濃度を測定した．その結果，それらは各PCB投与により両ラットで著しく低下した．このとき，Wistar系ラットにおいて，T_4の代謝を促進するUGT1 s，UGT1A1，UGT1A6の発現量およびT_4-UDP-GT活性は顕著に増加した．一方，Gunnラットではそれらに変化はまったく認められなかった(図6・1)．これらの結果から，Gunnラットにおいて，ペンタCBあるいはKC500を投与した後の血中T_4濃度の低下は，肝臓のT_4-UDP-GT活性の増加に依存しないことが示唆された．さらに，Wistar系ラットにPCBを投与したときの血中T_4濃度の低下も，少なくとも一部T_4-UDP-GTが非関与の機序による可能性が示唆された[5]．

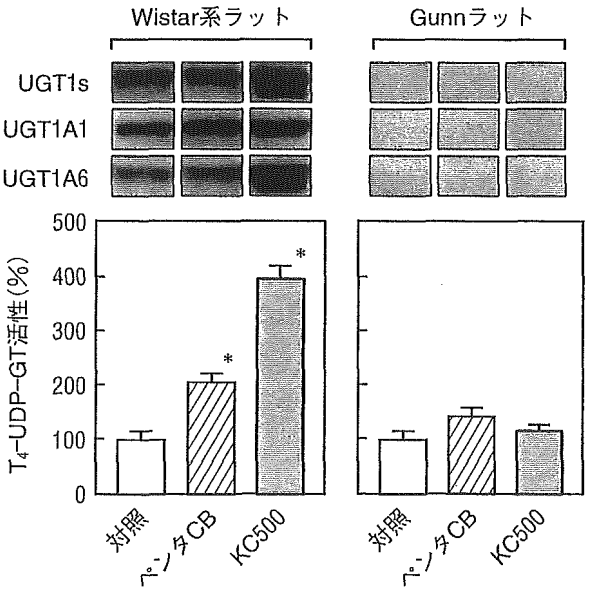

図6・1　Wistar系ラットおよびGunnラットにペンタCBおよびKC500を投与した後の肝ミクロソームのUGT分子種の発現量およびT_4-UDP-GT活性．平均±標準誤差．$n=4\sim6$．$^*p<0.05$．

T_4の代謝を亢進させる生体内反応として，T_4のグルクロン酸抱合のほかに，脱ヨウ素化反応が知られている．そこで，4種の動物にペンタCB，ヘキサCB，KC500を投与し，肝臓のI型ヨードサイロニン脱ヨウ素化酵素活性を測定した．しかし，いずれの場合にも，この酵素活性の増加は認められなかった．Aroclor1254を用いて類似した結果も報告されている．したがって，PCBによる血中T_4濃度の低下にI型ヨードサイロニン脱ヨウ素化酵素は関与していないと考えられる．

6. 4. 血中T_4濃度の低下に対するT_4とトランスサイレチンとの結合阻害の関与

特定のPCBおよびそのヒドロキシル化体は血中T_4の輸送タンパクであるトランスサイレチン(TTR)と競合的に結合する．詳細なメカニズムは明らかにされていないが，それらとTTRとの結合が血中T_4の標的器官への輸送を撹乱し，血中T_4濃度を低下させる一因となることが報告されている[6,7]．そこで，4種の動物にKC500を投与し，投与後4日目に[^{125}I]T_4を静脈内投与し，血中[^{125}I]T_4と血中TTRあるいはアルブミンとの結合率を測定した．いずれの動物でも対照群では，[^{125}I]T_4はほとんどTTRと結合していた．マウスでは，KC500投与により，いずれのタンパクとの結合にも変化はまったく認められなかった．ハムスターでは，KC500(100 mg/kg)投与により，[^{125}I]T_4とTTRとの結合

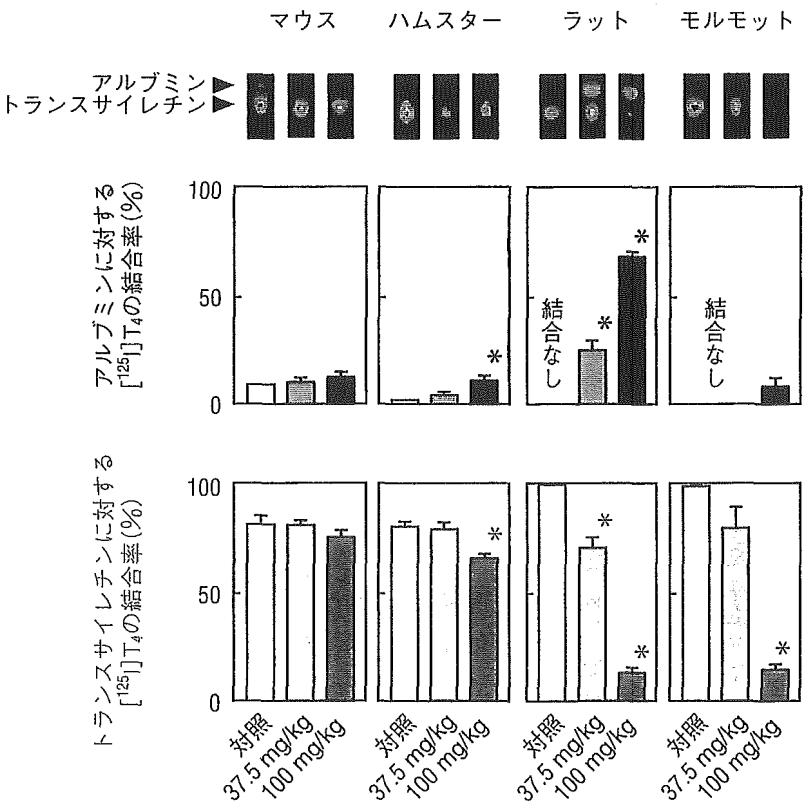

図6・2 Wistar系ラットにKC500を投与した後の[^{125}I]T_4と血中タンパク質との結合率．平均±標準誤差．n=3～4.*p<0.05(口絵11)．

率はわずかに減少した．一方，ラットおよびモルモットでは，KC500投与により，[^{125}I]T_4とTTRとの結合率は用量依存的に減少し，代わって[^{125}I]T_4とアルブミンとの結合率が増加した．この増加はラットにおいて顕著であった(図6・2，口絵11参照)．これらの結果から，ラットおよびモルモットでは，KC500によりT_4とTTRの結合阻害が起こっていることが示唆され，それが原因で，血中T_4濃度が低下した可能性が考えられる．一方，マウスでは，KC500により，T_4とTTRの結合阻害が起こっているとは考えにくく，血中T_4濃度の低下は，他のメカニズムによりひき起こされている可能性が示唆された．

6．5．甲状腺への直接作用，メチルスルフォン代謝物あるいはT_4と甲状腺ホルモン受容体との結合阻害の関与

PCBによる血中T_4濃度の低下の要因として，甲状腺濾胞上皮細胞におけるT_4の合成系の抑制，あるいは甲状腺からT_4の放出の抑制も考えられる．しかし，4種の動物にペンタCB，ヘキサCBあるいはKC500(それぞれED_{50})を投与したとき，甲状腺の腔胞変性，濾胞上皮細胞の肥大および過形成は，対照群と同程度であった．各PCBの今回用いた用量による血中T_4濃度の低下には，甲状腺への直接作用は考えにくい．

3‐メチルスルフォニル(3-$MeSO_2$-)および4-$MeSO_2$-ペンタCB，および3-$MeSO_2$-ヘキサCBなどのPCBのメチルスルフォン代謝物は，UGT1A1/6を誘導することにより，血中T_4の代謝を亢進し，血中T_4濃度の低下をひき起こす[8]．そこで，各PCB投与による4種の動物の血中T_4濃度の低下に，メチルスルフォン代謝物が関与しているか否かを検討した．しかし，3種のPCBを投与したとき，各動物の血中T_4濃度の低下と血中あるいは肝臓中メチルスルフォン代謝物濃度との間には相関はみられなかった．

また，PCBは甲状腺ホルモン受容体(TR)を介する遺伝子発現を抑制することにより，甲状腺ホルモンの撹乱をひき起こすことが報告されている[9]．そこで，6種のPCB，16種の$MeSO_2$-PCBおよび20種のヒドロキシル化PCBとT_4とのTRへの競合的結合能を調べた．しかし，検討したPCBおよびPCB代謝物のなかにはTRへ結合するものを見出すことはできなかった[10]．

6．6．血中T_4の肝臓への移行とトランスポーターの関与

これまでの検討から，PCBによる血中T_4濃度の低下の作用機序について十分に説明することは困難であった．そこで，T_4の体内動態に注目してさらに検討を加えた．マウス，ハムスター，ラットあるいはモルモットにKC500を投与し，投与後4日目に[^{125}I]T_4を静脈内投与し，血中からの[^{125}I]T_4の消失速度を測定した．血中の[^{125}I]T_4の消失速度は，[^{125}I]T_4の投与後5分から増加し，T_4の全身クリアランスおよび分布容積は，用量依存的に増加した(表6・1)．また，C57Bl/6系マウスに異なる

表6・1　マウス，ハムスター，ラットおよびモルモットにKC500を投与した後の[^{125}I]T_4の薬物動態パラメーター

動物	処置	用量 (mg/kg)	全身クリアランス (ml/min)	分布容積 (ml)
マウス	対照		0.016 ± 0.003	4.8 ± 0.3
	KC500	37.5	0.015 ± 0.002	4.9 ± 0.3
	KC500	100	0.024 ± 0.003*	6.8 ± 0.5*
ハムスター	対照		0.034 ± 0.004	11.9 ± 1.0
	KC500	37.5	0.059 ± 0.009*	25.4 ± 1.7*
	KC500	100	0.086 ± 0.008*	43.7 ± 5.0*
ラット	対照		0.074 ± 0.007	14.4 ± 0.4
	KC500	37.5	0.143 ± 0.019	30.9 ± 4.0*
	KC500	100	0.241 ± 0.046*	61.2 ± 5.4*
モルモット	対照		0.085 ± 0.017	34.7 ± 3.8
	KC500	37.5	0.120 ± 0.027	56.6 ± 7.6*
	KC500	100	0.216 ± 0.019*	66.9 ± 7.3*

平均±標準誤差．n=4～6.*p<0.05.

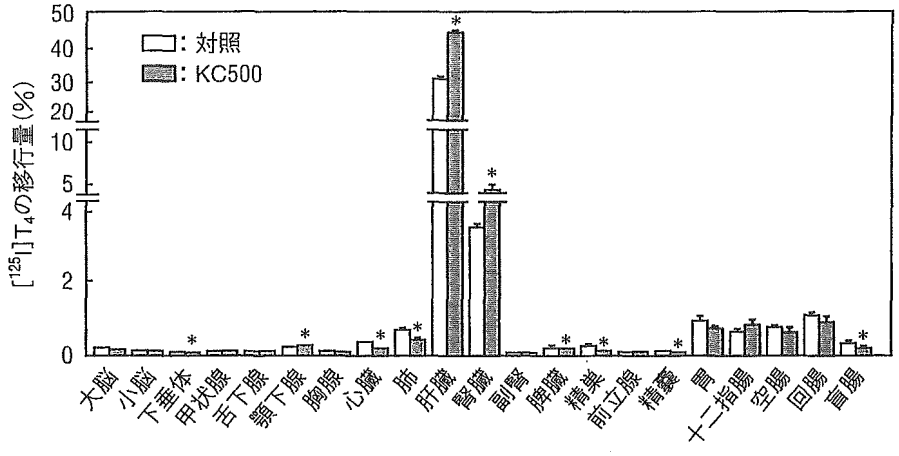

図6・3　KC500を処置したラットに，[^{125}I]T_4を静脈内投与した5分後の[^{125}I]T_4の組織分布．平均±標準誤差．n=4.*p<0.05.

タイプのPCB(3,3',4,4' - テトラクロロビフェニル，2,3',4,4',5 - ペンタクロロビフェニル，2,2',4,4',5,5'-ヘキサクロロビフェニル[非ダイオキシン様PCB])を投与し，同様の検討を試みたところ，いずれの場合にも血中T_4濃度は低下し，T_4の分布容積は増加した．これらの結果から，各動物にPCBを投与したとき，血中T_4濃度の低下は，血中から組織へのT_4の急速な移行によることが示唆された．そこで，血中から消失した[^{125}I]T_4がどこの組織に移行したかを明らかにするために，ラットにKC500を投与し，投与後4日目に[^{125}I]T_4を静脈内投与し，その5分後に各組織への[^{125}I]T_4の移行量を測定した．対照ラットの肝臓への[^{125}I]T_4の移行量は他の組織への移行量に比較して著しく多く，KC500投与により，その移行量は投与量の58%に増加した(図6・3)．また，KC500を処置したマウス，ハムスターおよびモルモットにおいても，肝臓への[^{125}I]T_4の移行量は，他の組織に比較して顕著に増加した．さらに，マウス，ハムスターおよびラットにフェノバルビタール(PB)を投与

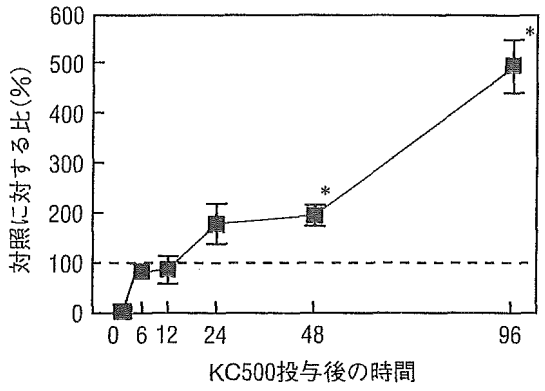

図6・4　ラットにKC500を投与した後の肝臓のLAT1のmRNAの発現量．平均±標準誤差．$n=4\sim5$．$^*p<0.01$．

し，血中T_4濃度が低下するとき，T_4の全身クリアランスおよび分布容積は増加し，肝臓へのT_4の移行量は増加した．これらの結果から，用いた動物において，ダイオキシン様PCB(Ah受容体依存性の毒性発現をするPCB)および非ダイオキシン様PCB(PB response unit依存性の毒性発現をするPCB)ともに，PCB投与による血中T_4濃度の低下は，T_4の分布容積が増加すること，すなわちT_4が血中からすみやかに肝臓に移行することに起因することが示唆された．

最近，甲状腺ホルモンを基質とするトランスポーターが次々と明らかにされている．その例としては，有機アニオン輸送ポリペプチド(Oatp1～4)，Na^+/タウロコール酸共輸送ペプチド(Ntcp)，L型アミノ酸トランスポーター(LAT1～2)，モノカルボン酸トランスポーター(MCT8)があげられる．これらのうち，Oatp1～4，NtcpおよびMCT8はラットの肝臓に発現していること，肝臓内へのT_4の輸送に関与していることが報告されている．そこで，ラットにKC500を投与し，経時的に肝臓を摘出し，各トランスポーターのmRNAの発現量を測定した．KC500を処置したラット肝臓のOatp2 mRNAの発現量は，処置後4日目に1.4倍に増加した．また，LAT1 mRNAの発現量は，処置後2日目から有意に増加し，4日目には5.0倍に増加した(図6・4)．これらの結果は，肝臓のLAT1およびOatp2の発現増加が，血中から肝臓へのT_4の移行量の増加をもたらす要因になっている可能性を示唆している．

6. 7. おわりに

これまでの多くの研究から，PCBによるラット血中T_4濃度の低下は，甲状腺における甲状腺ホルモンの合成・放出を抑制させること，甲状腺ホルモンの代謝クリアランスを促進させる(特にT_4-UDP-GTの誘導)こと，甲状腺ホルモンの末梢組織への移行(TTRを介するT_4の輸送)に異常をきたすことによってひき起こされることが報告されてきた．ところが，マウス，ハムスター，ラットおよびモルモットにペンタCB，ヘキサCBあるいはKC500を投与したとき，血中T_4濃度の低下は，甲状腺への直接作用，肝臓のT_4-UDP-GTおよび脱ヨウ素化酵素の誘導あるいはメチルスルフォン代謝物によるT_4の代謝促進，あるいはT_4とTRとの結合阻害では説明することが困難であった．そこで，PCBを投与した後，T_4の体内動態について検討したところ，PCBによる血中T_4濃度の低下は，血中

から肝臓へのT_4の移行量の増加に起因している可能性が示唆された．各PCBによる血中から肝臓へのT_4の移行量の違いは，各PCBのヒドロキシル化代謝物の生成量と，生成したヒドロキシル化代謝物とTTRとの親和性の強さ，また肝臓の甲状腺ホルモントランスポーターの発現量の増加割合などに依存する可能性が考えられる．また，血中から肝臓へのT_4の輸送のメカニズムは，PCBのタイプあるいは動物種により異なり，いくつかのT_4の輸送メカニズムが組み合わさっているものと考えられる．また，PCBによる胆汁中へのT_4のグルクロン酸抱合体の排泄量の変動は，肝臓へのT_4の移行量の違いと，T_4-UGP-GTの誘導の程度により左右され，血中T_4濃度の低下とは直接的な関連性は低いかもしれない．このように，PCBによる血中T_4濃度の低下機序やその動物種差を，単一の要因で説明することは難しく，これまでに検討してきた要因，あるいは未知の要因が複雑に絡み合って，各動物の血中T_4濃度の低下が惹起されるものと考えられる．今後，ヒトを含む多くの動物種のPCBによる血中甲状腺ホルモン濃度の減少に対する感受性を理解するために，末梢組織(特に肝臓)および脳における甲状腺ホルモンの取り込みメカニズム，甲状腺ホルモントランスポーターおよび甲状腺ホルモン応答遺伝子の機能とそれらの変動メカニズムについてさらに研究する必要がある．

参考文献

1. Agency for Toxic Substances and Disease Registry (2000) Toxicoligical profile for polychlorinated biphenyls (PCBs). Department of Health and Human Services, Public Health Service, Atlanta, GA, U.S.
2. Koopman-Esseboom C, Morse DC, Weisglas-Kuperus N, Lutke-Schipholt IJ, Van der Paauw CG, Tuinstra LGMT, Brouwer A, Sauer PJJ (1994) Effects of dioxins and polychlorinated biphenyls on thyroid hormone status of pregnant women and their infants. Pediatr. Res. 36:468-473
3. Craft ES, De Vito MJ, Crofton KM (2002) Comparative responsiveness of hypothyroxinemia and hepatic enzyme induction in Long-Evans rats versus C57BL/6J mice exposed to TCDD-like and phenobarbital-like polychlorinated biphenyl congeners. Toxicol. Sci. 68:372-380
4. Kato Y, Haraguchi K, Yamazaki T, Ito Y, Miyajima S, Nemoto K, Koga N, Kimura R, Degawa M (2003) Effects of polychrorinated biphenyls, Kanechlor-500, on serum thyroid hormone levels in rats and mice. Toxicol. Sci. 72:235-241
5. Kato Y, Ikushiro S, Haraguchi K, Yamazaki T, Ito Y, Suzuki H, Kimura R, Yamada S, Inoue T, Degawa M (2004) A possible mechanism for decrease in serum thyroxine level by polychlorinated biphenyls in Wistar and Gunn rats. Toxicol. Sci. 81:309-315
6. Cheek AO, Kow K, Chen J, McLachlan JA (1999) Potential mechanisms of thyroid disruption in humans: Interaction of organochlorine compounds with thyroid receptor, transthyretin, and thyroid-binding globulin. Environ. Health Perspect. 107:273-278
7. Meerts IATM, Assink Y, Cenijn PH, Van Den Berg JH, Weijers BM, Bergman Å, Koeman JH, Brouwer A (2002) Placental transfer of a hydroxylated polychlorinated biphenyl and effects on fetal and maternal thyroid hormone homeostasis in the rat. Toxicol. Sci. 68:361-371
8. Kato Y, Haraguchi K, Shibahara T, Shinmura Y, Masuda Y, Kimura R (2000) The induction of hepatic microsomal UDP-glucuronosyltransferase by the methylsulfonyl metabolites of polychlorinated biphenyl congeners in rats. Chem.-Biol. Interact. 125:107-115
9. Iwasaki T, Miyazaki W, Takeshita A, Kuroda Y, Koibuchi N (2002) Polychlorinated biphenyls suppress thyroid hormone-induced transactivation. Biochem. Biophys. Res. Commun. 299:384-388
10. Gauger KJ, Kato Y, Haraguchi K, Lehmer H-J, Robertson LW, Bansal R, Zoeller RT (2004) Polychlorinated biphenyls (PCBs) exert thyroid hormone-like effects in the fetal rat brain but do not bind to thyroid hormone receptors. Environ. Health Perspect. 112:516-523

BMC Genomics

BioMed Central

Methodology article

Open Access

"Per cell" normalization method for mRNA measurement by quantitative PCR and microarrays

Jun Kanno*†[1], Ken-ichi Aisaki†[1], Katsuhide Igarashi[1], Noriyuki Nakatsu[1], Atsushi Ono[1], Yukio Kodama[1] and Taku Nagao[2]

Address: [1]Division of Cellular and Molecular Toxicology, National Institute of Health Sciences, 1-18-1, Kamiyoga, Setagaya-ku, Tokyo 158-8501, Japan and [2]President, National Institute of Health Sciences, 1-18-1, Kamiyoga, Setagaya-ku, Tokyo 158-8501, Japan

Email: Jun Kanno* - kanno@nihs.go.jp; Ken-ichi Aisaki - aisaki@nihs.go.jp; Katsuhide Igarashi - igarashi@nihs.go.jp; Noriyuki Nakatsu - n-nakatsu@nihs.go.jp; Atsushi Ono - Atsushi@nibio.go.jp; Yukio Kodama - kodama@nihs.go.jp; Taku Nagao - nagao@nihs.go.jp

* Corresponding author †Equal contributors

Published: 29 March 2006

*BMC Genomics*2006, 7:64 doi:10.1186/1471-2164-7-64

Received: 06 November 2005
Accepted: 29 March 2006

This article is available from: http://www.biomedcentral.com/1471-2164/7/64

Abstract

Background: Transcriptome data from quantitative PCR (Q-PCR) and DNA microarrays are typically obtained from a fixed amount of RNA collected per sample. Therefore, variations in tissue cellularity and RNA yield across samples in an experimental series compromise accurate determination of the absolute level of each mRNA species per cell in any sample. Since mRNAs are copied from genomic DNA, the simplest way to express mRNA level would be as copy number per template DNA, or more practically, as copy number per cell.

Results: Here we report a method (designated the "Percellome" method) for normalizing the expression of mRNA values in biological samples. It provides a "per cell" readout in mRNA copy number and is applicable to both quantitative PCR (Q-PCR) and DNA microarray studies. The genomic DNA content of each sample homogenate was measured from a small aliquot to derive the number of cells in the sample. A cocktail of five external spike RNAs admixed in a dose-graded manner (dose-graded spike cocktail; GSC) was prepared and added to each homogenate in proportion to its DNA content. In this way, the spike mRNAs represented absolute copy numbers per cell in the sample. The signals from the five spike mRNAs were used as a dose-response standard curve for each sample, enabling us to convert all the signals measured to copy numbers per cell in an expression profile-independent manner. A series of samples was measured by Q-PCR and Affymetrix GeneChip microarrays using this Percellome method, and the results showed up to 90 % concordance.

Conclusion: Percellome data can be compared directly among samples and among different studies, and between different platforms, without further normalization. Therefore, "percellome" normalization can serve as a standard method for exchanging and comparing data across different platforms and among different laboratories.

Background

Normalization of gene expression data between different samples generated in the same laboratory using a single platform, and/or generated in different geographical

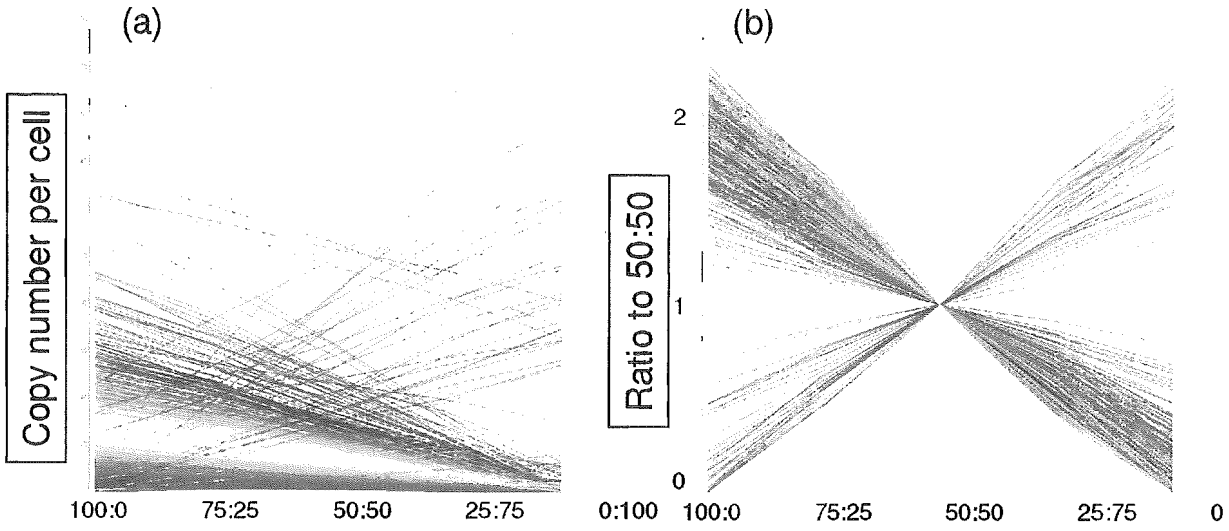

Figure 1

Dose-response linearity check by LBM. Dose-response linearity of the Affymetrix GeneChip by the LBM (liver-brain mix) sample set. Five samples, i.e. mixtures of mouse liver and brain at ratios of 100:0, 75:25, 50:50, 25:75 and 0:100, were spiked with GSC and measured by Affymetrix GeneChips Mouse430-2. Signals were normalized by the Percellome method as described in the text. Line graphs are in (a) copy numbers and (b) ratio to 50:50 sample for the top 1,000 probe sets with coefficient of correlation (R^2) closest to 1 among those having 1 copy or more per cell in the 50:50 sample (19,979 probe sets out of 45,101). The number of probe sets with $R^2 > 0.950$ was 8,655, and $R^2 > 0.900$ was 11,719.

regions using multiple platforms, is central to the establishment of a reliable reference database for toxicogenomics and pharmacogenomics. Transforming expression data into a "per cell" database is an effective way of normalizing expression data across samples and platforms. However, transcriptome data from the quantitative PCR (Q-PCR) and DNA microarray analyses currently deposited in the database are related to a fixed amount of RNA collected per sample. Variations in RNA yield across samples in an experimental series compromise accurate determination of the absolute level of each mRNA species per cell in any sample. Normalization against housekeeping genes for PCRs, and global normalization of ratiometric data for microarrays, is typically performed to account for this informational loss. Additional methods, such as the use of external mRNA spikes, reportedly improve the quality of data from microarray systems. For example, Holstege et al. [1] described a spike method against total RNA, based on their finding that the yields of total RNA from wild type and mutant cells were very similar. Hill et al. [2] reported a spike method against total RNA for normalizing hybridization data such that the sensitivities of individual arrays could be compared. Lee et al. [3] demonstrated that "housekeeping genes" cannot be used as a reference control, and van de Peppel et al. [4] described a normalization method of mRNA against total RNA using an external spike mixture. To achieve satisfactory performance they used multiple graded doses of external spikes, covering a wide range of expression, in order to align the ratiometric data by Lowess normalization [5]. Hekstra et al. [6] presented a method for calculating the final cRNA concentration in a hybridization solution. Sterrenburg et al. [7] and Dudley et al. [8] reported the use of common reference control samples for two-color microarray analyses of the human and yeast genomes, respectively. These are pools of antisense oligo sequences against all sense oligos present on the microarray. Instead of antisense oligos, Talaat et al. [9] used genomic DNA as a common reference control in studies of *E. coli*. Statistical approaches have been proposed for ratiometric data to improve inter-microarray variations, especially of non-linear relations [10]. However, because control samples may differ among studies, ratiometric data cannot easily be compared across multiple studies unless a common reference, such as a mixture of all antisense counterparts of spotted sense sequences is used [7-9]. Nevertheless, as long as the normalization is calibrated to total RNA, variations in total RNA profile cannot be effectively cancelled out. Although

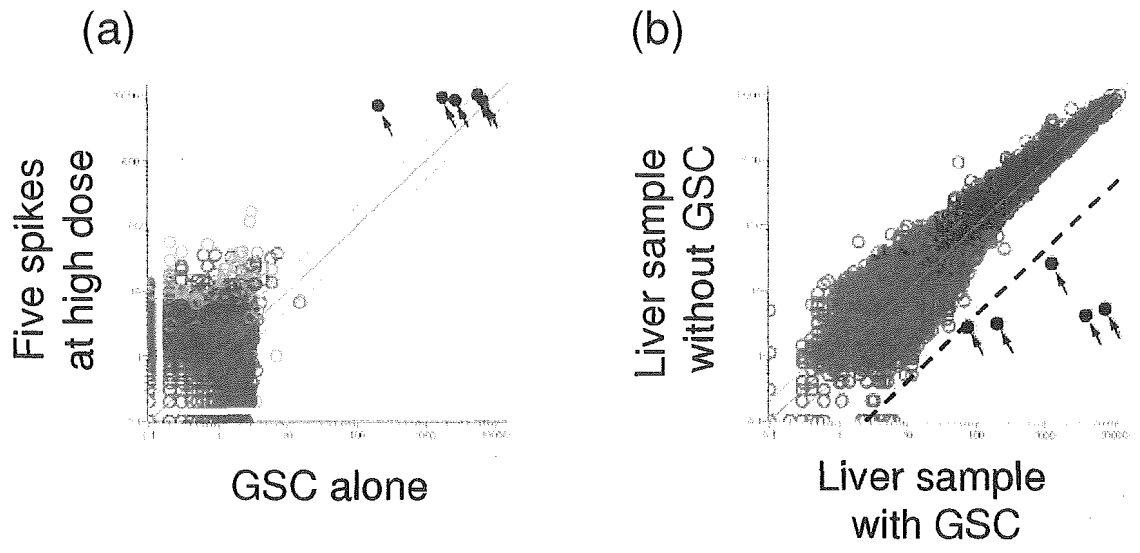

Figure 2
Cross-hybridization of GSC. Cross-hybridization of the GSC spike mRNAs to Affymetrix GeneChip. (a) A scatter plot of a blank sample with the GSC (horizontal axis) and a blank with the five spike RNAs at a high dosage (vertical axis) measured by MG-U74v2A GeneChips (raw values generated by Affymetrix MAS 5.0 software). The five spikes are indicated by black dots with arrows. Signals of the murine probe sets were below 20 on the horizontal axis, indicating negligible cross-hybridization of GSC spike mRNAs to the murine probe sets. (b) A scatter plot of a liver sample with GSC (horizontal axis) and without GSC (vertical axis) measured by MG-U74v2A GeneChips. The five spikes are again indicated by black dots with arrows. The dotted line is the 1/25 fold (4%) line. Cross-hybridization of mouse liver mRNAs to the GSC signals was considered negligible (less than 4%).

some of these reports share the idea that "absolute expression" and "transcripts per cell" should entail robust normalization, further practical development to enable universal application has been awaited.

Here, we report a method for normalizing expression data across samples and methods to the cell number of each sample, using the DNA content as indicator. This normalization method is independent of the gene expression profile of the sample, and may contribute to transcriptome studies as a common standard for data comparison and interchange.

Results

Dose-response linearity of the measurement system as a basis for the Percellome method

The fidelity of transcript detection is the key to this "per cell" based normalization method, which generates transcriptome data in "mRNA copy numbers per cell". The Q-PCR system was tested by serially diluting samples to confirm the linear relationship between Ct values and the log of sample mRNA concentration (data not shown). High density oligonucleotide microarrays from Affymetrix [11] were used in our experiments. We tested the linearity of the Affymetrix GeneChips using a set of five samples made of mixtures of liver and brain in ratios of 100:0, 75:25, 50:50, 25:75, and 0:100 (designated "LBM" for liver-brain mix). The results showed a linear relationship ($R^2 > 0.90$) between fluorescence intensity and input for a sufficient proportion of probe sets, i.e. about 37% of the probe sets in the older MG-U74v2 and 70% in the newest Mouse Genome 430 2.0 GeneChip were above the detection level (approximately one copy per cell) in the 50:50 sample (Figure 1) [see Additional files 1 and 2].

Dose-response linearity alone is not sufficient to generate true mRNA copy numbers. An important additional requirement is that the ratio of signal intensity to mRNA copy number should be equal among all GeneChip probe sets of mRNAs and PCR primers. The Q-PCR primer sets were designed to perform at similar amplification rates to minimize differences between amplicons. The melting

Table 1: The spike factors for various organs/tissues

Species	Organ/Tissue (adult, unless otherwise noted)	Spike Factor	total RNA/genomic DNA	SD
Mouse	Liver	0.2	211	46
Mouse	Lung	0.02	22	4
Mouse	Heart	0.05	-	-
Mouse	Thymus	0.01	8	2
Mouse	Colon Epitherium	0.05	105	30
Mouse	Kidney	0.1	-	-
Mouse	Brain	0.1	-	-
Mouse	Suprachiasmatic nucleus (SCN)	0.1	-	-
Mouse	Hypothalamus	0.1	63	4
Mouse	Pituitary	0.1	52	8
Mouse	Ovary	0.02	35	4
Mouse	Uterus	0.02	42	12
Mouse	Vagina	0.02	81	38
Mouse	Testis	0.15	56	7
Mouse	Epididymis	0.07	53	16
Mouse	Bone marrow	0.02	14	3
Mouse	Spleen	0.02	-	-
Mouse	Whole Embryo	0.15	97	36
Mouse	Fetal Telencephalon E10.5–16.5	0.1	48	9
Mouse	Neurosphere (E11.5–14.5)	0.03	42	10
Mouse	E9.5 embryo heart	0.15	58	15
Mouse	cell lines	0.2	-	-
Rat	Liver	0.2	-	-
Rat	Kidney	0.2	-	-
Rat	Uterus	0.04	56	5
Rat	Ovary	0.04	56	9
Human	Cancer Cell Lines	0.2	116	26
Xenopus	liver	0.03	-	-
Xenopus	embryo	0.15	-	-

temperature was set between 60° and 65°C with a product size of approximately 100 base pairs using an algorithm (nearest neighbor method, TAKARA BIO Inc., Japan), and the amplification co-efficiency (E) was set within the range 0.9 ± 0.1 (E = 2^{-(1/slope)}-1 on a plot of log2 (template) against Ct value). For the GeneChip system, the signal/copy performance of each probe set depended on the strategy of designing the probes to keep the hybridization constant/melting temperature within a narrow range, ensuring that the dose-response performances of the probe sets were similar (cf. http://www.affymetrix.com/technology/design/index.affx). Failing this, any differences should at least be kept constant within the same make/version of the GeneChip. Taking into consideration the biases that lead to imperfections in estimating absolute copy numbers in each gene/probe set, we developed normalization methods to set up a common scale for Q-PCR and Affymetrix GeneChip systems.

The grade-dosed spike cocktail (GSC) and the "spike factor" for the Percellome method

A set of external spike mRNAs was used to transfer the measurement of cell number in the sample (as reflected by its DNA content) to transcriptome analysis. For the spikes, we utilized five *Bacillus subtilis* mRNAs that were left open for users in the Affymetrix GeneChip series. The extent to which the *Bacillus* RNAs cross-hybridized with other probe sets was checked for the Affymetrix GeneChip system. The GSC was applied to Murine Genome U74Av2 Array (MG-U74v2) GeneChips with or without a liver sample. As shown in Figure 2, cross-hybridization between *Bacillus* RNAs and the murine gene probe sets was negligible [see Additional files 3 and 4]. Mouse Genome 430 2.0 Array (Mouse430-2), Mouse Expression Arrays 430A (MOE430A) and B (MOE430B), Rat Expression Array 230A (RAE230A), *Xenopus laevis* Genome Array and Human Genome U95Av2 (HG-U95Av2) and U133A (HG-U133A) Arrays sharing the same probe sets for these spike mRNAs showed no sign of cross-hybridization with the *Bacillus* probes (data not shown).

We prepared a cocktail containing in vitro transcribed Bacillus mRNAs in threefold concentration steps, i.e. 777.6 pM (for AFFX-ThrX-3_at), 259.4 pM (for AFFX-LysX-3_at), 86.4 pM (for AFFX-PheX-3_at), 28.8 pM (for AFFX-DapX-3_at) and 9.6 pM (for AFFX-TrpnX-3_at). By referring to the amount of DNA in a diploid cell and employing a "spike factor" determined by the ratio of

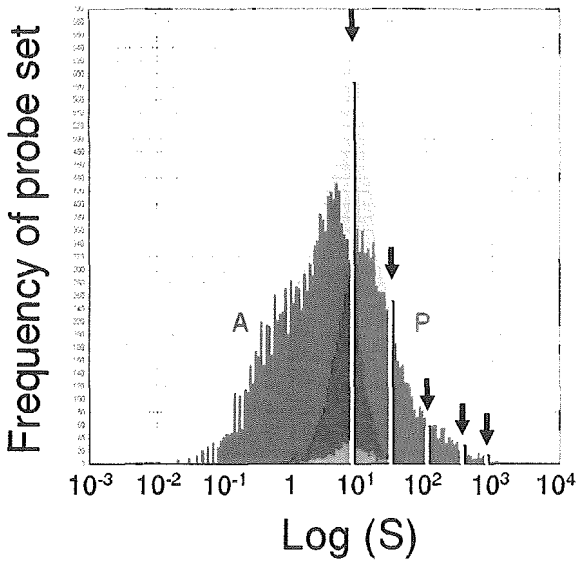

Figure 3
Positioning of GSC spike mRNAs in Affymetrix GeneChip dose-response range. A frequency histogram of the probe sets of Affymetrix GeneChip Mouse430-2 is shown. The histogram for all probe sets (gray) shows near-normal distribution. Blue columns are the "present" calls (P), red columns "absent" calls (A) and green "marginal" calls. The five yellow lines indicate the positions of the GSC spike mRNAs that are chosen to cover the "present" call range by a proper "spike factor".

total RNA to genomic DNA in a tissue type (Table 1), the spike mRNAs were calculated to correspond to 468.1, 156.0, 52.0, 17.3 and 5.8 copies per cell (diploid), respectively, for the mouse liver samples (spike factor = 0.2). The ratio of mRNAs in the cocktail is empirically chosen depending on the linear range of the measurement system and the available number of spikes. Here, we set the ratio to three to cover the "present" call probe sets of the Affymetrix GeneChip system (Figure 3).

We tested this grade-dosed spike cocktail (GSC) by Q-PCR and confirmed that the Ct values of the spike mRNAs were linearly related to the log concentrations (cf. Figure 4a), i.e. could be expressed as

$$Ct = \alpha \log C + \beta \quad \{1\}$$

The GSC was also tested by the GeneChip system and it was confirmed that the log of the spike mRNA signal intensities was linearly related to the log of their concentrations (cf. Figure 4b),

$$\log S = \gamma \log C + \delta \quad \{2\}$$

The linear relationship between the Ct values (Ct) and the log of RNA concentration (log C) was reasonable given the definition of Ct values (derived from the number of PCR cycles, i.e. doubling processes). The linear relationship between the log of GeneChip signal intensity (log S) and the log of RNA concentration (log C) was rationalized by the near-normal distribution of log S over all transcripts (cf. Figure 3).

Calculation of copy numbers of all genes/probe sets per cell

As described above, using a combination of DNA content and the spike factor of the sample, the GSC spike mRNAs become direct indicators of the copy numbers (C') per cell. When the samples were measured by Q-PCR or GeneChip analysis, the five GSC spike signals in each sample should obey function {1} for Q-PCR and function {2} for GeneChip with a good linearity. If the observed linearity was poor, a series of quality controls was performed and the measurement repeated. The coefficients of the functions were determined for each sample by the least squares method. Under the assumption that all genes/probe sets share the same signal/copy relationship, signal data for all genes/probe sets were fitted to the functions {1'} or {2'}, which are the individualized functions of {1} and {2} for each sample measurement (i).

$$Ct = \alpha i \log(C') + \beta i \quad \{1'\}$$

$$\text{Log } (S) = \gamma i \log(C') + \delta i \quad \{2'\}$$

(i = sample measurement no.)

The Q-PCR Ct values (Ct) and microarray signal values (S) of all mRNA species in the sample (i) are converted to copy numbers per cell (C') by the inverses of functions {1'} and {2'}, i.e. {3} and {4} below:

$$C' = B\text{^}((Ct-\beta i)/\alpha i) \quad \{3\}$$

for Q-PCR (Figure 4a).;

$$C' = B\text{^}((\log S-\gamma i)/\delta i) \quad \{4\}$$

for GeneChips (Figure 4b),

where B is the logarithmic base used in {1} and {2} (see Materials and Methods for details).

Real world performance of the Percellome method

The correspondence between Q-PCR and GeneChip was tested using a sample set from 2,3,7,8-tetrachlorodibenzodioxin (TCDD)-treated mice. Sixty male C57BL/6 mice

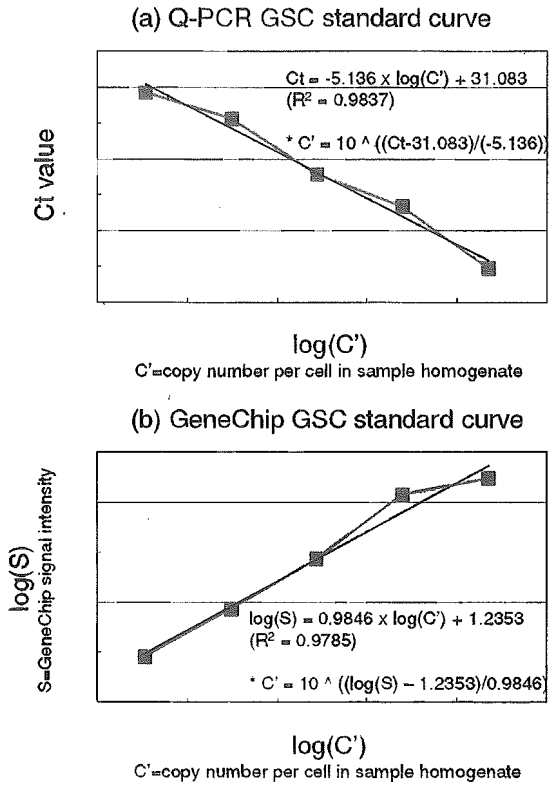

Figure 4
The dose-response linearity of the GSC spikes in Q-PCR and the Affymetrix GeneChip array system. Linear relationships are shown between (a) the Q-PCR Ct values and log of copy number (log (C')), and (b) the GeneChip log signal intensity (log(S)) and log of copy number (log (C')) of the GSC mRNAs. The regression functions were obtained by the least squares method. The inverse functions (*) were further used to generate the copy numbers of all other genes/probe sets for Percellome normalization.

were divided into 20 groups of 3 mice each. TCDD was administered once orally at doses of 0, 1, 3, 10 and 30 μg/kg, and the livers were sampled 2, 4, 8 and 24 h after administration. Nineteen primer pairs were prepared for Q-PCR and the Ct values of the liver transcriptome were measured. The same 60 liver samples were measured using the Affymetrix Mouse430-2 GeneChip [see Additional files 5 through 8 and 9 through 12]. Q-PCR and GeneChip data were normalized against cell number by functions {3} and {4}, respectively. The averages and standard deviations (sd) of each group (n = 3) were calculated and plotted as three layers of isoborograms on to 5

4 matrix three-dimensional graphs (Figure 5). Together with another sample set (data not shown), a total of thirty-six primer pairs were compared, and there was a correlation of up to 90% between the Q-PCR and GeneChip surfaces. It is notable that not only the average surfaces but also the +1sd and -1sd surfaces corresponded closely in shape and size. We infer that the differences resulted mainly from biological variations among the three animals in each experimental group rather than from measurement error (cf. Figure 7).

An important feature of Percellome normalization is its independence from the overall expression profile of the sample. When gene expression profiles differ among samples, Percellome normalization produces a robust transcriptome that is different from total-RNA dependent global normalization. As an example, Figure 6 shows the results of an experiment on the uterotrophic response of ovariectomized mice to estrogen treatment [12] [see Additional files 13 and 14]. The uteri of the vehicle control are atrophic because the ovaries, the source of intrinsic estrogens, are absent. The uteri of the treated groups are hypertrophic owing to estrogenic stimulus from the test compound administered. Global normalization (90 percentile) between the vehicle control group and the high-dose (1,000 mg/kg) group indicated that 4,600 of 12,000 probe sets showed 2-fold or greater increase, 470 were reduced by 0.5 or less, and 7,400 remained between these extremes. In contrast, analysis of Percellome-normalized data revealed that almost all the 12,000 probe sets showed a 2-fold or greater increase, including actin, GAPDH and other housekeeping genes. The hypertrophic tissues, consisting of cells with abundant cytoplasm, provide convincing evidence for the increases in various cellular components including housekeeping gene products.

Another important feature of Percellome normalization is the commonality of the expression scale across platforms. Batch conversion can be performed between results obtained from different platforms when the data are generated by the Percellome method. A practical strategy for such normalization is to prepare a set of samples from a target organ of interest with differences in gene expression, and measure them once by each platform. Data conversion functions with good linear dose-response relationships can be obtained individually for those genes/probe sets that are measured by both platforms (Figure 7).

Discussion

We have developed a novel method for normalizing mRNA expression values to sample cell numbers by adding external spike mRNAs to the sample in proportion to the genomic DNA concentration. For non-diploid or aneuploid samples, an average DNA content per cell should be determined beforehand for accurate adjustment. When there is significant DNA synthesis, a similar adjustment should be considered.

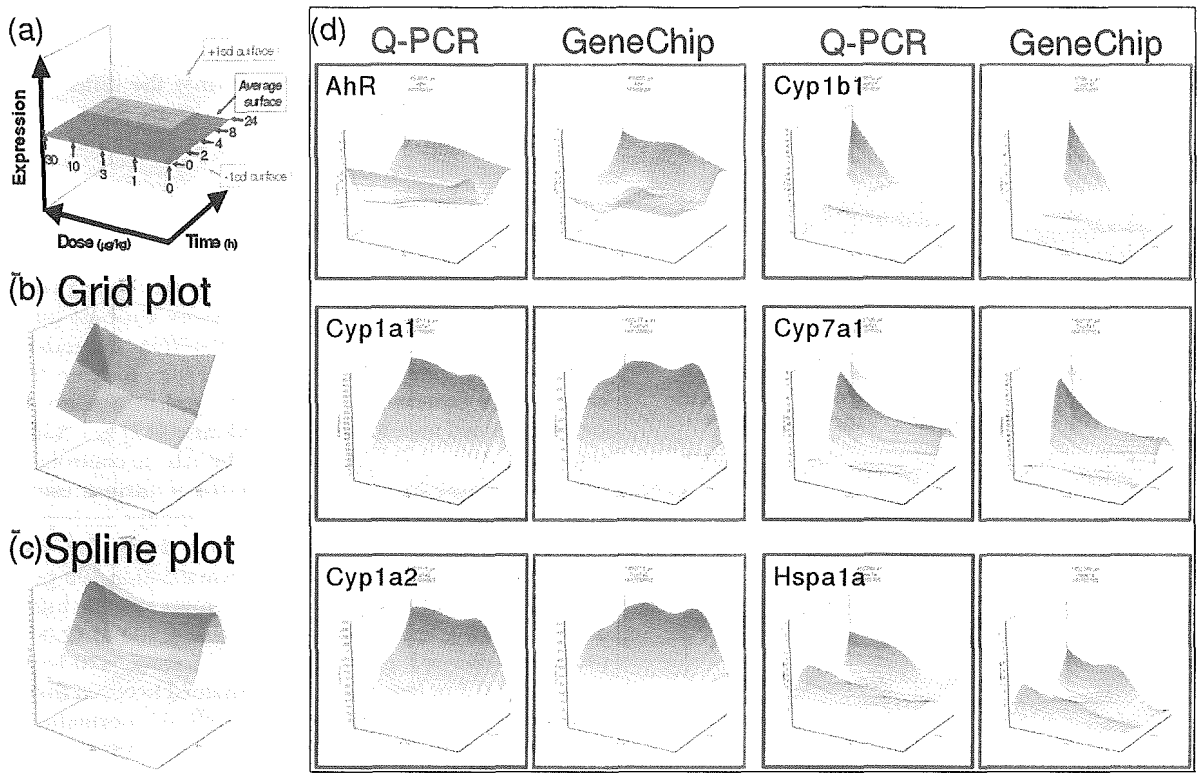

Figure 5

Correspondence between Q-PCR and GeneChip data. Sixty male C57BL/6 mice were divided into 20 groups of 3 mice each. 2,3,7,8-tetrachlorodibenzodioxin (TCDD) was administered once orally at doses of 0, 1, 3, 10 and 30μg/kg, and the liver was sampled 2, 4, 8 and 24 h after administration. The liver transcriptome was measured by the Affymetrix Mouse430-2 GeneChip. For Q-PCR, nineteen primary pairs were prepared and the Ct values of the same 60 liver samples were measured (19 genes and 5 spikes in duplicate, using a 96-well plate for 2 samples, total 30 plates). The Percellome data were plotted on to 3-dimensional graphs for average, +1sd, and − 1sd surfaces as shown in (a). The scale of expression (vertical axis) is the copy number per cell. The 0 h data (*) are copied from the 2 h/dose 0 point for better visualization of the changes after 2 h. The surfaces are demonstrated as a grid plot (b) where the grid points indicate one treatment group (n = 3), and a smoothened spline surface plot (c) for easier 3D recognition ((b), (c): Gys2 (glycogen synthase 2, 1424815_at) showing a typical circadian pattern. (d) the smoothened plots of 6 representative genes/ probe sets generated by Q-PCR (red) and GeneChip (blue). AhR (arylhydrocarbon receptor, 1450695_at) showed imperfect correspondence. Cyp1a1 (cytochrome P450, family 1, subfamily a, polypeptide 1, 1422217_a_at) and Cyp1a2 (1450715_at) showed good correlations between Q-PCR and GeneChip except for the saturation in GeneChips above c. 400 copies per cell. Cyp1b1 (1416612_at) and Cyp7a1 (1422100_at) showed good correspondence. Hspa1a (heat shock protein 1A, 1452888_at) showed fair correspondence despite low copy numbers, near the nominal detection limit of the Affymetrix GeneChip system.

The smallest sample to which we have successfully applied the direct DNA quantification method with sufficient reproducibility is the 6.75 dpc (days post coitus) mouse embryo which consists of approximately 5,000 cells. This sample size is also approximately the lower limit for double amplification protocol to obtain sufficient amount of RNA for Affymetrix GeneChip measurement (cf. http://www.affymetrix.com/Auth/support/downloads/manuals/expression_print_manual.zip.)

High-resolution technology such as laser-capture microdissection (LCM) has become popular and the average sample size analyzed is getting smaller. An alternative method for LCM samples is to count the cell number in the course of microdissection. Although we have not yet applied Percellome method to LCM samples, we have applied the alternative method to cell culture samples to gain Percellome data. Stereological and statistical calculations should become available to correct the number of partially sectioned cells in the LCM samples. Another issue for small samples is the yield of RNA. Approximately

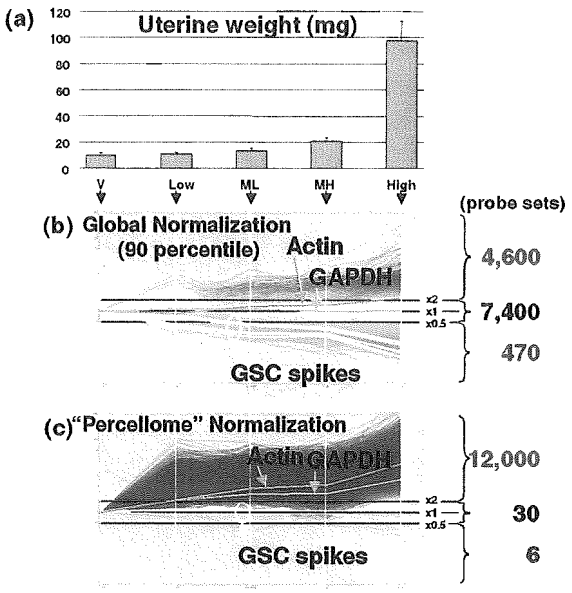

Figure 6
Uterotrophic response of ovariectomized female mice by an estrogenic test compound. (a) Shows the uterine weight, which increases in a dose-dependent manner; V, vehicle control; Low, low dose; ML, medium-low dose; MH, medium-high dose; High, high dose group. (b) Shows the line display of uterine gene expression (Affymetrix MG-U74v2 A GeneChips) normalized by global normalization (90 percentile), and (c) by the Percellome normalization. Averages of three samples per group were visualized (by K. A.). The five white lines are the GSC mRNAs. The green and blue lines are actin (AFFX-b-ActinMur/M12481_3_at) and GAPDH (glyceraldehyde-3-phosphate dehydrogenase, AFFX-GapdhMur/M32599_3_at), respectively. By global normalization, 7,400 probe sets remained unchanged and 4,600 probe sets increased more than two-fold in the H group compared to the V group, whereas almost all probe sets measured had increased. It is noted that housekeeping genes such as actin and GAPDH are significantly induced on a per cell basis.

30 ng of total RNA is retrieved from a single 6.75 dpc mouse embryo. This amount is sufficient for a double amplification protocol (DA) to prepare enough RNA for an Affymetrix GeneChip measurement. An inherent problem with the DA data is that the gene expression profile differs from that of the default single amplification protocol (SA). Consequently the DA percellome data differ from that of SA as if they were produced by a different platform. To bridge the difference, we applied the procedure that was used for data conversion between Q-PCR and GeneChip (cf. Figure 7). A set of spiked-in standard samples including the LBM sample set (of sufficient concentration) were measured by the SA protocol and diluted versions to the limit measured by the DA protocol. These data provided us with information about whether DA was successful as a whole (by comparing 5' signal to 3' signals of selected probe sets) and which probe sets were properly amplified by DA (by checking the linearity of the diluted LBM data). For those probe sets that proved to be linearly amplified, conversion functions between DA and SA were generated. These details, along with embryo expression data will be published elsewhere.

Figures 5 and 7 indicate a close correspondence between the data generated by Q-PCR and GeneChip analyses. Since each of the 60 samples was normalized individually against each GSC signal, the high similarity between the two platforms indicates the robustness and stability of this spike system (cf. Figure 7, Cyp7a1 data). Although more spikes could potentially increase the accuracy of normalization, our experience is that five spikes are practically sufficient for covering the detection range of GeneChip microarrays and Q-PCR, as long as they are used in combination with the "spike factor". The overall benefits of using a minimum number of external spikes include lower probability of cross-hybridization, a reduced number of wells and spots occupied by the spikes in the Q-PCR plates and small scale microarrays, and less effort in preparation, QC and supply.

The Percellome data can be truly absolute when all mRNA measurements including GSC spikes are strictly proportional to the original copy numbers in the sample homogenate. As noted earlier, this condition is not guaranteed by any platform despite linearity of response. Therefore, the Percellome-normalized values have some biases for each primer pair/probe set, depending on the steepness of the dose-response curves. An advantage of Percellome normalization is that, as long as such biases are consistently reproduced within a platform, the data can be compared directly among samples/studies on a common scale. Consequently, when a true value is obtained by any other measure, all the data obtained in the past can be simultaneously batch-converted to the true values.

This batch-conversion strategy can be extended to data conversion between different versions and different platforms, as long as the data are generated in copy numbers "per cell". We have shown an example between Affymetrix GeneChip and Q-PCR for limited numbers of probe sets (cf. Figure 7). Custom microarrays that accept our GSC for Percellome normalization are in preparation by Agilent Technologies (single color) and GE Healthcare (CodeLink Bioarray).

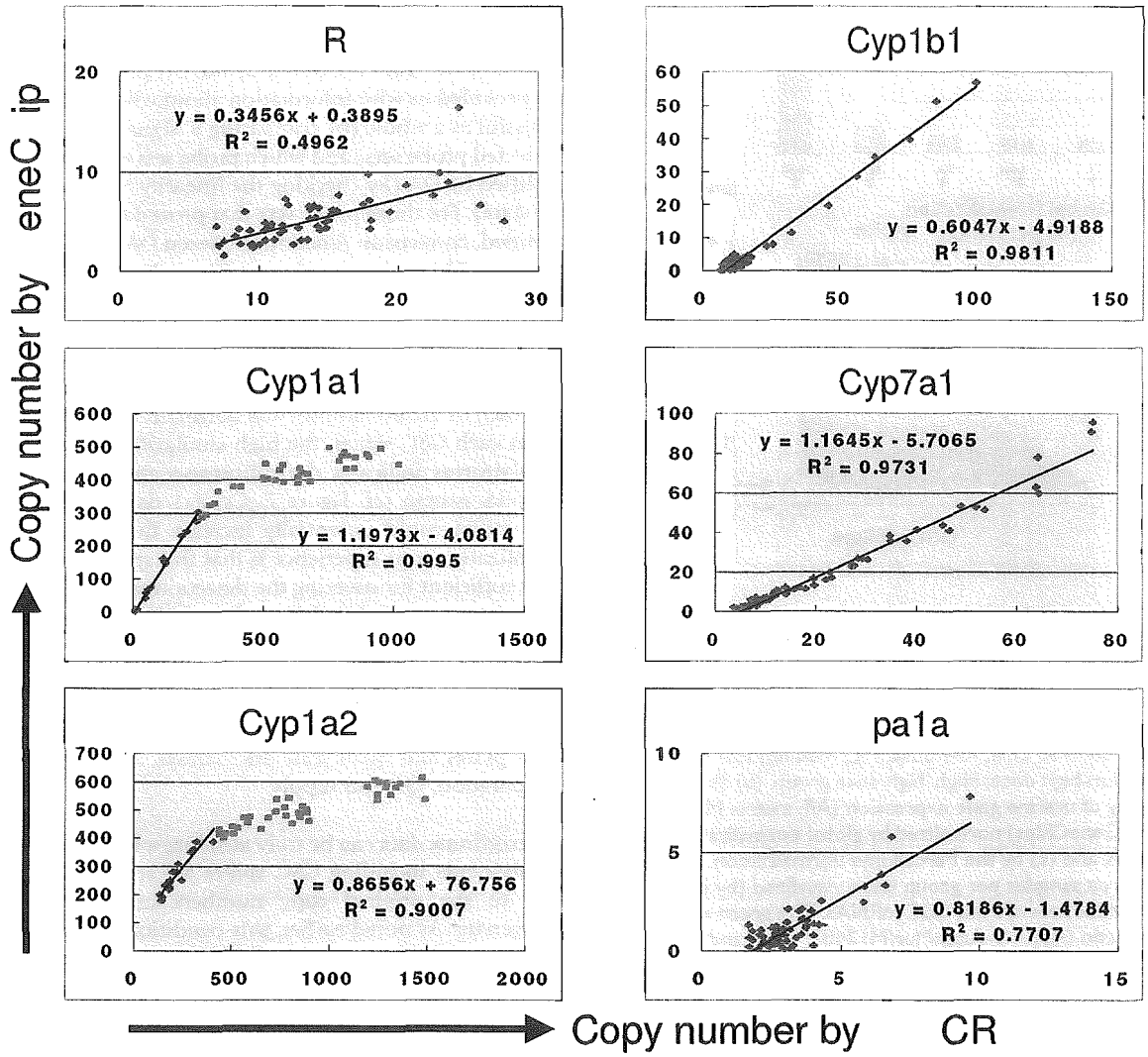

Figure 7

Conversion functions between Q-PCR and GeneChip. The data shown in Figure 5 as 3D surfaces are shown as a scatter plot (60 plots). The regression function can be used to convert Q-PCR to GeneChip and vice versa, with a level of certainty indicated by coefficient of correlation. It is noted that Cyp1a1 and Cyp1a2 became saturated above about 400 copies per cell in GeneChip system (indicated in pink plots). Cyp7a1 showed high linearity, indicating that the variation shown by the split +1sd and -1sd surfaces in Figure 5 reflected biological (animal) variation, not measurement errors.

Another important contribution of Percellome analysis is in the area of archived data in private and public domains. Firstly, Percellome data are the result of a simple linear transformation of the raw microarray data; preserving the distribution and order of the probe set data. Therefore, parametric or non-parametric methods should be able to align the data distribution and generate estimates of mRNA copy number of the non-spiked archival samples. Any archival samples that are re-measurable by Percellome method will greatly increase the accuracy of estimation. Secondly, percellome can provide appropriate bridging information between old and new versions of Affymetrix GeneChips, such as human HU-95 and HU-133, murine MU-74v2 and MOE430 series. This should also facilitate comparisons between newly generated and archived data.

The Percellome method was developed for a large-scale toxicogenomics project [13] using the Affymetrix GeneChip system. It was intended to compile a very large-scale database of comprehensive gene expression profiles in response to various chemicals from a series of experiments conducted over an extended time period. However, the method also proved to be useful for small-scale platforms such as 96 well plate-based Q-PCRs as shown above, and probably for small-scale targeted microarrays. In both cases, highly inducible or highly transcribed genes are likely to be selected. Therefore, the expression profiles may differ significantly among samples such that profile-dependent normalization (e.g. global normalization) may not be applicable. In such cases, the profile-independent nature of the Percellome method provides a robust normalization.

To demonstrate the profile-independence of the Percellome method, we chose an extreme case – the uterotrophic response assay (cf. Figure 6). The treated uteri were composed of hypertrophic cells with abundant cytoplasm whereas the untreated uteri were composed of hypoplastic cells with scant cytoplasm. This indicates that the uteri of untreated ovariectomized mice were quiescent, and that a majority of the inducible genes were probably transcriptionally inactive. Therefore, the identification of most genes as being induced by 2-fold or greater is reasonable and expected. In most *in vivo* experiments, the gene profiles of the samples are much more similar. However, there is always a set of genes that is found to be "increased" when analyzed on a "per one cell" basis that are declared to be "decreased" by global type normalization, or vice versa. Such increase/decrease calls made by the global type normalization can differ according to the normalization parameters. In both cases, the Percellome method can inform the researcher how much the expression profiles are distorted by the treatment, such as in the case of the uterotrophic assay. We also note that *in vitro* experiments such as cell-based studies tend to generate data similar to that of uterotrophic experiment.

Conclusion

Percellome data can be compared directly among samples and among different studies, and between different platforms, without further normalization. Therefore, "percellome" normalization can serve as a standard method for exchanging and comparing data across different platforms and among different laboratories. We hope that the Percellome method will contribute to transcriptome-based studies by facilitating data exchanges among laboratories.

Methods

Animal experiments

C57BL/6 Cr Slc (SLC, Hamamatsu, Japan) mice maintained in a barrier system with a 12 h photoperiod were used in this study. For the liver transcriptome experiments, twelve week-old male mice were given a single dose of the test compound by oral gavage, and the liver was sampled at 2, 4, 8 and 24 h post-gavage. For the uterotrophic experiment, 6 week old female mice were ovariectomized 14 days prior to the 7 day repeated subcutaneous injection of a test compound [12]. Animals were euthanized by exsanguination under ether anesthesia and the target organs were excised into ice-cooled plastic dishes. Tissue blocks weighing 30 to 60 mg were placed in an RNase-free 2 ml plastic tube (Eppendorf GmbH., Germany) and soaked in RNAlater (Ambion Inc., TX) within 3 min of the beginning of anesthesia. Three animals per treatment group were used and individually subjected to transcriptome measurement.

Sample homogenate preparation

The tissue blocks soaked in RNAlater were kept overnight at 4°C or until use. RNAlater was replaced in the 2 ml plastic tube with 1.0 ml of RLT buffer (Qiagen GmbH., Germany), and the tissue was homogenized by adding a 5 mm diameter Zirconium bead (Funakoshi, Japan) and shaking with a MixerMill 300 (Qiagen GmbH., Germany) at a speed of 20 Hz for 5 min (only the outermost row of the shaker box was used).

Direct DNA quantitation

Three separate 10 μl aliquots were taken from each sample homogenate to another tube and mixed thoroughly. A final 10 μl aliquot therefrom was treated with DNAse-free RNase A (Nippon Gene Inc., Japan) for 30 min at 37°C, followed by Proteinase K (Roche Diagnostics GmbH., Germany) for 3 h at 55°C in 1.5 ml capped tubes. The aliquot was transferred to a 96-well black plate. PicoGreen fluorescent dye (Molecular Probes Inc., USA) was added to each well, shaken for 10 seconds four times and then incubated for 2 min at 30°C. The DNA concentration was measured using a 96 well fluorescence plate reader with excitation at 485 nm and emission at 538 nm. λ phage DNA (PicoGreen Kit, Molecular Probes Inc., USA) was used as standard. Measurement by this PicoGreen method and the standard phenol extraction method correlated well (coefficient of correlation = 0.97, data not shown). The smallest sample size for reproducible and reliable DNA quantitation is about 5,000 cells that corresponds to a 6.75 dpc mouse embryo.

The grade-dosed spike cocktail (GSC)

The following five *Bacillus subtilis* RNA sequences were selected from the gene list of Affymetrix GeneChip arrays (AFFX-ThrX-3_at, AFFX-LysX-3_at, AFFX-PheX-3_at, AFFX-DapX-3_at, and AFFX-TrpnX-3_at) present in the MG-U74v2, RG-U34, HG-U95, HG-U133, RAE230 and MOE430 arrays: thrC, thrB genes corresponding to nucleotides 248–2229 of X04603; lys gene for diami-